ceramics

MDPI

Article

Ceramic Filters for the Efficient Removal of Azo Dyes and Pathogens in Water

Marvellous Oaikhena [1,2], Abimbola E. Oluwalana-Sanusi [1,2], Puseletso P. Mokoena [1], Nonhlangabezo Mabuba [3], Themba Tshabalala [1,*] and Nhamo Chaukura [1,*]

[1] Advanced Materials Research Group, Department of Physical and Earth Sciences, School of Natural and Applied Sciences, Sol Plaatje University, Kimberley 8300, South Africa; 202220930@spu.ac.za (M.O.); abimbola.oluwalana@spu.ac.za (A.E.O.-S.); puseletso.mokoena@spu.ac.za (P.P.M.)
[2] Risk and Vulnerability Science Centre, Sol Plaatje University, Private Bag X5008, Kimberley 8300, South Africa
[3] Department of Chemical Sciences, University of Johannesburg, Johannesburg 2092, South Africa; nmabuba@uj.ac.za
* Correspondence: themba.tshabalala@spu.ac.za (T.T.); nhamo.chaukura@spu.ac.za (N.C.)

Abstract: Overcoming the scarcity of safe and sustainable drinking water, particularly in low-income countries, is one of the key challenges of the 21st century. In these countries, the cost of centralized water treatment facilities is prohibitive. This work examines the application of low-cost ceramic filters as point-of-use (POU) devices for the removal of methylene blue, o-toluidine blue, *Staphylococcus aureus*, and *Salmonella typhi* from contaminated water. The ceramic filters had typical kaolinite functional groups, making them suitable for the removal of dyes and pathogens. Surface charge measurements indicated strongly anionic filters, while thermal properties confirmed the carbonization of the biowaste additive leaving behind a porous kaolinite structure which subsequently dehydroxylated into meta kaolinite. In addition, morphological data showed heterogeneous filter surfaces. Increased biomass content improved the permeability, water adsorption, flow rate, and apparent porosity of the filter. The ceramic filter removed methylene blue (42.99–59.74%), o-toluidine (79.95–92.71%), *Staphylococcus aureus* (98–100%), and *Salmonella typhi* (75–100%). Overall, the study demonstrated the effectiveness of POU ceramic filters in removing organic pollutants in contaminated water while serving as disinfectants.

Keywords: biowaste; clay; environmental pollution; filtration; water flow rate

check for updates

Citation: Oaikhena, M.; Oluwalana-Sanusi, A.E.; Mokoena, P.P.; Mabuba, N.; Tshabalala, T.; Chaukura, N. Ceramic Filters for the Efficient Removal of Azo Dyes and Pathogens in Water. *Ceramics* **2023**, *6*, 2134–2147. https://doi.org/10.3390/ceramics6040131

Academic Editor: Francesco Baino

Received: 9 September 2023
Revised: 23 October 2023
Accepted: 2 November 2023
Published: 9 November 2023

Correction Statement: This article has been republished with a minor change. The change does not affect the scientific content of the article and further details are available within the backmatter of the website version of this article.

Copyright: © 2023 by the authors. Licensee MDPI, Basel, Switzerland. This article is an open access article distributed under the terms and conditions of the Creative Commons Attribution (CC BY) license (https://creativecommons.org/licenses/by/4.0/).

1. Introduction

Less than 1% of the water on Earth is potable, and the rest is contaminated by pollutants from various activities such as agriculture, manufacturing, energy generation, and mining. These anthropic activities release contaminants such as pesticides, heavy metals, halide ions, dyes, herbicides, medicines, and detergents, into aquatic systems [1,2]. Every year, especially in LICs, more than 500,000 children die from waterborne illnesses [3]. According to the World Health Organization, low-income countries account for more than 99.8% of global deaths due to the consumption of contaminated drinking water [4]. Hence, there is a need for safe drinking water provision.

Azo dyes, such as methylene blue (MB) and ortho-toluidine blue (*o*-TB), can occur in industrial effluents, and are resistant to photodegradation, microbial degradation, and washing-induced fading [5]. Consequently, they persist in the environment and pose public health risks such as genotoxicity, mutagenicity, and carcinogenicity [5]. In addition to the contamination by azo dyes discharged into water bodies, pathogens are also a major concern. Various pathogenic organisms can be found in wastewater, posing a serious health danger. Public health risks arising from waterborne diseases and microbial contamination are a growing concern. The microbial contamination of aquatic systems can arise from human and animal fecal matter, as well as the indiscriminate release of polluted health

care and domestic effluents. These introduce enteric pathogens, such as *Clostridium difficile*, Shigella species, Polio virus, parasitic protozoans (e.g., *Cryptosporidium* spp.), helminths (e.g., *Trichuris trichiura*), and different strains *of Escherichia coli*, into aquatic systems [6,7]. When these pathogens are consumed, they can cause waterborne diseases such as diarrhea, cholera, dysentery, and typhoid. Accordingly, the removal of microbiological organisms from water is imperative.

Various techniques such as biodegradation, advanced oxidation processes, disinfection, filtration, adsorption, coagulation, and solar disinfection have been used for the treatment of azo dye- and pathogen-contaminated wastewater [8–10]. Ultrafiltration, nanofiltration, and reverse osmosis have also proved effective in removing azo dyes and other dissolved contaminants [11]. However, microfiltration and ultrafiltration processes are energy intensive, and can only be used as pre-processing stages [12,13]. Filtration is generally a simple and effective method of treating contaminated aquatic systems [14]. It holds great promise for safe drinking water provision, especially in low-income countries. Additionally, it can be adapted for point-of-use (POU) in water treatment applications [15]. Ceramic filters (CFs), membrane filters, bios and filters, and candle filters are some examples of POU water filtration systems [16].

In many developing countries, the provision of safe drinking water is a challenge, due to the associated economic and social costs [17]. Considering the large population without access to safe drinking water, several POU treatment systems have been introduced for the treatment of contaminated water [14]. In this regard, CFs have proved effective and efficient for the removal of colloidal particles and various chemical and pathogenic pollutants in contaminated water at household level [18]. These simple systems involve filtration of water through a porous ceramic media, which are commonly fabricated from clay and biomass to produce pot-like devices with pores that selectively retain large particles [19]. Ceramic filters present such benefits as high thermal and mechanical durability, high hydrophilicity, well-defined porosity, anti-bacterial activity, high flux even at low pressures, and efficient separation [20].

The goal of this study was to develop and assess the performance of low-cost CFs for the removal of MB, *o*-TB, *S. aureus*, and *S. typhi* from contaminated water, through the use of locally sourced clay and waste coffee bean residue to generate well defined pores in fabricated CF. The results suggest that CFs can potentially be useful in POU water treatment to improve water quality for household treatment in areas with inadequate centralized water treatment facilities.

2. Materials and Methods

2.1. Materials

Methylene blue ($C_{16}H_{18}ClN_3S$) and toluidine blue ($C_{15}H_{16}N_3S^+$) were purchased from Merck (Modderfontein, South Africa) and used without further purification. *S. aureus* and *S. typhi* were obtained from Inqaba Laboratories (Pretoria, South Africa). Waste coffee bean residues were sourced from local coffee shops, and clay was obtained from a local village.

2.2. Fabrication of Ceramic Filters

Ceramic filters were fabricated from a mixture of clay and coffee bean residues in different proportions following a previously described method [19], as presented in Table 1. The mixture was thoroughly mixed for homogeneity by adding water in small portions and mixing until a smooth dough was obtained.

Table 1. The composition of ceramic filters.

Ceramic Filters	Coffee Bean Residues (*w*/*w*%)	Clay (*w*/*w*%)
CF-25	25	75
CF-30	30	70
CF-35	35	65
CF-40	40	60

The dough was subsequently placed in a custom-made wooden mold and compacted by a hydraulic press to produce uniformly shaped wet CFs. Thereafter, the wet CFs were dried for 7 days in ambient conditions before being fired in a muffle furnace at 600 °C and a heating rate of 20 °C/min for 2 h, and subsequently ramped to 900 °C and held for 4 h [20] (Figure 1).

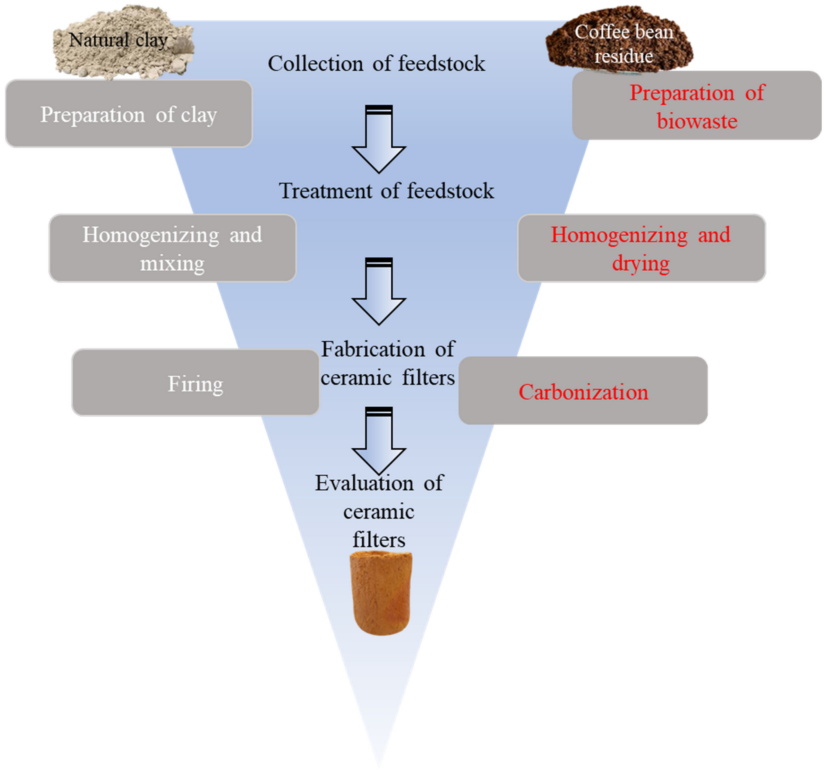

Figure 1. The fabrication process of ceramic filters.

2.3. Characterization of Feedstock and Ceramic Filters

The clay and coffee bean residues were dried and characterized to investigate their surface functional groups, crystallinity, surface morphology, elemental composition, and thermal stability. The infrared spectra for the coffee bean residues, clay, and ceramic filters before and after filtration, were collected using an FTIR spectrometer (PerkinElmer FT-IR UATR two Midrand, South Africa) in the wavenumber range of 400–4000 cm^{-1}. The crystallinity was analyzed using an X-ray diffractometer (XRD) (Panalytical X-PertPro, Malvern Pananalytical, Randburg, South Africa) operated at 40 kV and 40 mA with monochromatic Cu Kα radiation at λ = 1.54060. The surface morphology and elemental composition were characterized using a scanning electron microscope (SEM) (JEOL JSM-7800F, Tokyo, JAPAN) coupled to an energy-dispersive X-ray spectrometer (EDS), in the thermal field emission mode under a vacuum of 9.634×10^{-5} Pa. The BET surface area, and pore volume were measured by a N_2 porosimeter (Autosorb iQ3, Quanta chrome, Boynton Beach, FL, USA) at 77 K after a 2 h outgas at 373.15 K. To investigate the thermal stability of the starting materials and ceramic filters, a thermal gravimetric analyzer (TGA) and differential thermal analyzer (DTA) (Perkin Elmer, TGA-8000, Midrand, South Africa) operated at a constant heating rate of 10 °C/min from 50 to 900 °C under oxygen, were used.

2.4. Physical Characterization of Ceramic Filters

2.4.1. Apparent Porosity

To determine apparent porosity (p) (Equation (1)), the weight of dry CF (w_d) was obtained. The mass of the CF floating in water (w_w) was then determined by weighing it after it had been soaked in boiling water for 2 h [19].

$$p = \frac{w_w + w_d}{w_s + w_w} \quad (1)$$

where w_s is weight of saturated CF.

2.4.2. Water Absorption and Water Flow Rate

The dry weight of CF was determined, and the CF was then soaked in distilled water for 24 h to ascertain the water absorption (w_{ab}) (Equation (2)). After 24 h, the CFs were minimally dried with a paper towel and reweighed to determine their wet weight (w_w).

$$w_{ab} = \frac{w_w - w_d}{w_d} \times 100 \quad (2)$$

The water flow rate (F), which serves as indicator for permeability, was calculated using Equation (3). The volume of water (V) that drained over a predetermined time (t) from a filter that was initially full was used to calculate the permeability.

$$F = \frac{V}{t} \quad (3)$$

2.5. Evaluation of the Capacity of CFs to Remove Methylene Blue and Ortho-Toluidine Blue

The capacity of the CFs to remove MB and *o*-TB from contaminated water were evaluated following established methods. Briefly, 80 mg/L (80 ppm) each of MB and *o*-TB and were transferred into volumetric flasks and made up to 400 mL with distilled water. MB and *o*-TB are cationic dyes with a pH of 3.2 and 4, respectively. The dye solution was then passed through the CFs and the permeate collected at 2 min intervals, and the filtration cycle repeated four times for MB and five times for *o*-TB. The permeate was collected over different times depending on the water flow rate. Thus, 20 min for CF-25, 10 min CF-30, 8 min CF-35, and 120 s for CF-40. The concentration of the dye in the feed solution (C_0) and the concentration of the residual dye in the permeate (Cp) were determined using a UV-Vis spectrophotometer (Shimadzu UV-1800, Chicago, USA), from which the removal efficiency (ε) was calculated (Equation (4)).

$$\in = \frac{C_0 - C_p}{C_0} \quad (4)$$

2.6. Evaluation of the Ceramic Filters for Pathogens Removal

All the glassware used for the antibacterial assessment experiments were sterilized at 121 °C for 15 min using an autoclave (Hirayama, Model: HV-5 0, Kasukabe-Shi Saitama Japan). A loopful of each of *S. aureus* and *S. typhi* was separately inoculated in 100 mL of nutrient broth in a 250 mL Erlenmeyer flask and incubated (SANYO CO_2 Incubator, Model: MCO-17AI, Tokyo, Japan) at 37 °C overnight. Distilled water was spiked with a stock culture of *S. aureus* and *S. typhi* separately to produce feed water, which was then passed through the CFs individually. The feed water and permeate (1 mL each) were separately plated on nutrient agar using the pour plate method and incubated at 37 °C overnight. The initial feed water was diluted using sterilized distilled water to obtain 10^{-2} dilution feed, which were subsequently treated the same way as the initial feed water. To evaluate the performance of the CFs, colony forming units (cfu/mL) (Equation (5)) were used for

quantitative estimation, and visual microscopy images for qualitative assessment. The overall effectiveness of the CFs in removing pathogens was computed using Equation (6).

$$\text{CFU} = \frac{\text{Colony number} \times \text{Dilution factor}}{\text{Volume of sample}} \quad (5)$$

$$\text{r} = \frac{\text{CFU}_{\text{before}} - \text{CFU}_{\text{after}}}{\text{CFU}_{\text{before}}} \quad (6)$$

2.7. Evaluation of Recyclability of CFs for Repeated Use

The stability of CF was evaluated by performing recyclability tests. After each filtration process, each CF was washed several times with distilled water, dried in the oven at 120 °C for 4 h, and calcined at 500 °C in the muffle furnace before the next cycle. This was performed for 4 cycles for MB, and 5 cycles for *o*-TB.

3. Results

3.1. Physico-Chemical Characteristics of Clay, Coffee Bean Waste, and Ceramic Filters

3.1.1. Surface Functional Groups

The FTIR spectrum for clay had kaolinite attributes (Figure 2a). Specifically, the peaks at 3600 cm^{-1}, 3100 cm^{-1}, and 1631 cm^{-1}, are attributable to the stretching and bending vibrations of OH and H_2O, respectively, which are common to kaolinite [21]. The Si-O vibration appeared at 1200 cm^{-1}, the Si-O-Si group of the tetrahedral sheet at 1000 cm^{-1}, while the Al-O bending appeared at 572 cm^{-1}. These bands closely resemble those found in heterogenous kaolinite. The FTIR spectra for CFs after usage (Figure 2a insert), showed minimal redshift of the Si-O-Si, Si-O, and Al-O peaks. The interaction of the metal oxides with the azo dyes and the pathogen is expected to produce a change in the peak positions. However, in this study, the results were inconclusive.

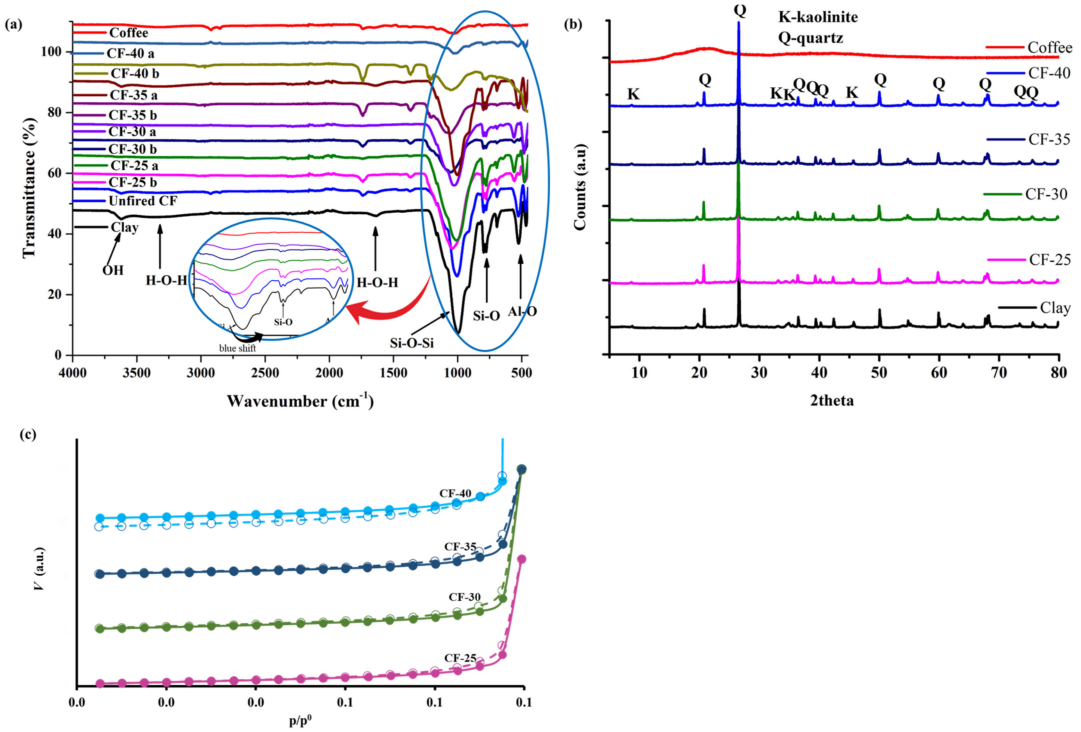

Figure 2. (**a**) FTIR, (**b**) XRD spectra, for clay, coffee bean residue, and ceramic filters, and (**c**) BET isotherms for CF-25, CF-30, CF-35, and CF-40.

The FTIR spectrum for coffee bean residue showed peaks between 3400 cm^{-1} and 3000 cm^{-1}, attributed to the O-H stretching, which is likely due to inter- and intramolecular

hydrogen bonding with polymetric hydrocarbons such phenols, carboxylic acids, and alcohols [22]. The presence of free OH groups and bonded O-H bands of carboxylic acid is indicated by this O-H stretching vibration, which occurs over a wide range of frequencies [23]. The two sharp peaks at 2935 cm^{-1} and 2854 cm^{-1}, which are due to the asymmetric and symmetric stretching of C-H bonds in aliphatic chains, respectively, are evidence of the existence of sp^3 and sp^2 hybridized carbons [22]. These peaks have been linked to the level of caffeine in coffee [24]. Overall, the surface functional groups on coffee bean residues are typical of biomass-based materials.

The FTIR spectrum of the ceramic filters fabricated with variable coffee bean residues and clay content exhibited peaks for both materials. However certain peaks, such as Si-O-Si and Si-O, were shifted from 1049 cm^{-1} and 857 cm^{-1} to 1049 cm^{-1} and 793 cm^{-1}, respectively, while O-H and C-H peaks were eliminated after firing. These changes in peaks could be due to the counterions connected to carboxylate and OH moieties, which are the major groups involved in the uptake of metal ions.

3.1.2. XRD Analysis

Figure 2b shows the XRD patterns of clay, ceramic filters and coffee beans. The peaks observed in the pristine clay and ceramic filters of 2θ at 21°(100), 26°(011), 36°(110), 39°(102), 40°(111), 42°(200), 50°(003), 60°(121), 68°(031), 73°(104), 76°(302), and 77°(220) indicate the presence of the quartz phase corresponding to ICDD:04-008-7651, while the peaks at 12°(001), 33°(020), 34°(110), and 45°(111) indicate the presence of the kaolinite phase corresponding to ICDD:01-083-0971. These peaks are well-fitted with the powder diffraction data of heterogenous phase of quartz and kaolinite from previous studies [25–28]. The XRD analysis reveals that the clay contains Si-O from silica. Kaolinite clay has been reported to consist of quartz (SiO_2) in higher percentage of 64%, while Al_2O_3, K_2O, and MgO occurs at 25.2%, 2.47%, and 1.58%, respectively [29], which can account for the intense peaks of quartz detected in the XRD pattern. The amorphous characteristics of coffee bean residues are also shown. The high background intensity indicates the presence of highly disordered carbon with the distinctive broad humps at 23.5° and 43°, typical of amorphous carbonaceous materials [24].

3.1.3. Textural Properties of the Ceramic Filters

The N_2 sorption isotherms exhibit a type III hysteresis loop (Figure 2c), which is typical for porous materials characterized by a narrow pore size distribution [30]. For CF25, CF30, and CF35, the BET surface area ranged from 6.2 to 7.9 m^2/g, while the pore diameter and volume were in the ranges of 1.50–2.50 nm and 0.06–0.09 cm^3/g, respectively. The BET surface area for CF40 was 35.3 m^2/g, and the pore diameter and pore volume were 142.3 nm and 2.51 cm^3/g, respectively. Although the other filters did not show a definite trend, as expected, the high coffee bean waste content in CF40 increased the pore dimensions and overall porosity. Thus, the water flow rate and apparent porosity are relatively higher than the other filters. The presence of multifunctional groups—such as SiO_2, Al_2O_3, traces of iron oxide, and inorganic elements coupled with high specific area and porous structure—makes the CF crucial as a high-quality adsorbent.

3.1.4. Surface Morphology of Ceramic Filters

The SEM micrographs of the CFs show a heterogeneous morphology and high densification (Figure 3). The images also show the porous nature of the CFs, which likely affects the permeability, water flow rate, and selectivity [31]. This determines their suitability for the removal of MB, *o*-TB, *S. aureus*, and *S. typhi*. The SEM images of CF-25 (Figure 3a) and CF-30 (Figure 3b) showed voids formed from the calcination of coffee bean residue. Images for CF-35 showed a flay-like pattern (Figure 3c), while CF-40 showed dense and irregular morphology (Figure 3d). In addition, the SEM images showed increasing biomass content resulted in a rougher filter surface. Therefore, the different morphological properties exhibited by the CFs might influence their filtration properties. The distribution composition

data show a uniform distribution of elements such as Si, Al, Na, Mg, Ca, C, O, Fe, and K in the CFs. These most likely arise from the components of kaolinite, which are mainly silicon oxide, aluminum oxide, traces of iron oxide, and inorganic elements [29]. The presence of carbon could be attributed to trapped carbonaceous compounds derived from coffee bean residues produced during firing [19].

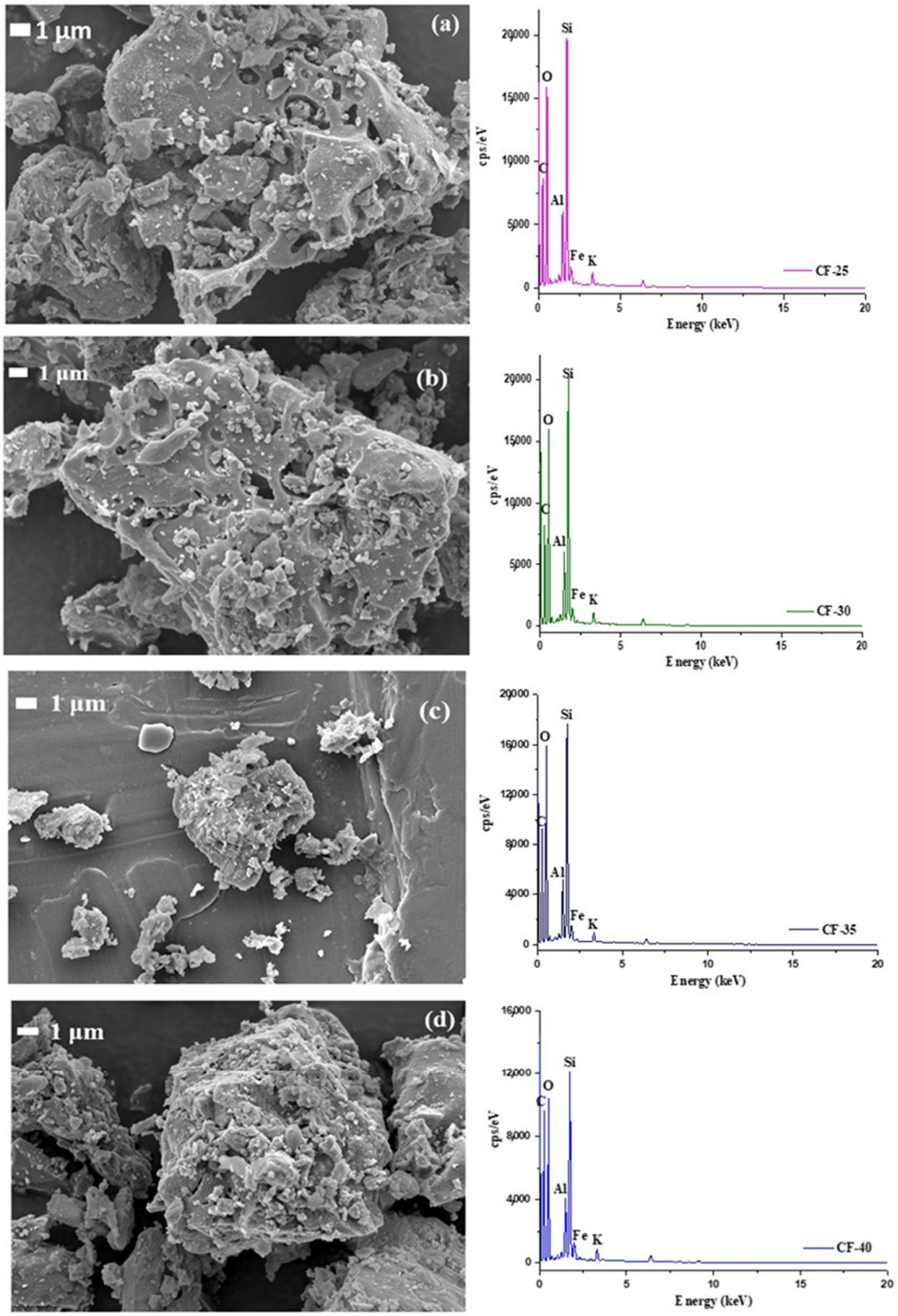

Figure 3. SEM images and the corresponding EDX spectra and elemental maps (inserts) for (**a**) CF-25, (**b**) CF-30, (**c**) CF-35, and (**d**) CF-40.

3.1.5. The Thermal Stability of Ceramic Filters

The TGA-DTA curves for the CFs are shown in Figure 4. The CFs showed a total mass loss of about 35% for CF-25 (Figure 4a), 36% for CF-30 (Figure 4b), 49% for CF-35 (Figure 4c), and 57% for CF-40 (Figure 4d) within the temperature range of 50 °C–850 °C. The variation of weight loss results in shrinkage of the CFs. The peak at 98 °C corresponds to the elimination of the moisture and interlayer water [30], while the peak around 300 °C is ascribed to the decomposition of organic matter and dehydration of clay. Below 400 °C, the mass loss is caused by the removal of the primary volatile materials, such as coffee bean residues, whereas the endothermic peaks at 550 and 650 °C can be attributed dihydroxylation of kaolinite as it transforms into meta kaolinite [32]. Nevertheless, at above 540 °C, marginal weight losses were observed (CF-25 had 0.8% weight loss, CF-30 lost 0.8%, while CF-35 was 0.9% and CF-40 was 1.0%), and this was attributed to the thermal stability of kaolinite. The meta kaolinite particles hold the platelet shape of the kaolinite. The endothermic peaks at 780 °C and 880 °C can be attributed to decomposition of dolomite and calcite, respectively [30]. Overall, to enhance the creation of meta kaolinite, sintering temperatures higher than 700 °C are appropriate for ceramic applications.

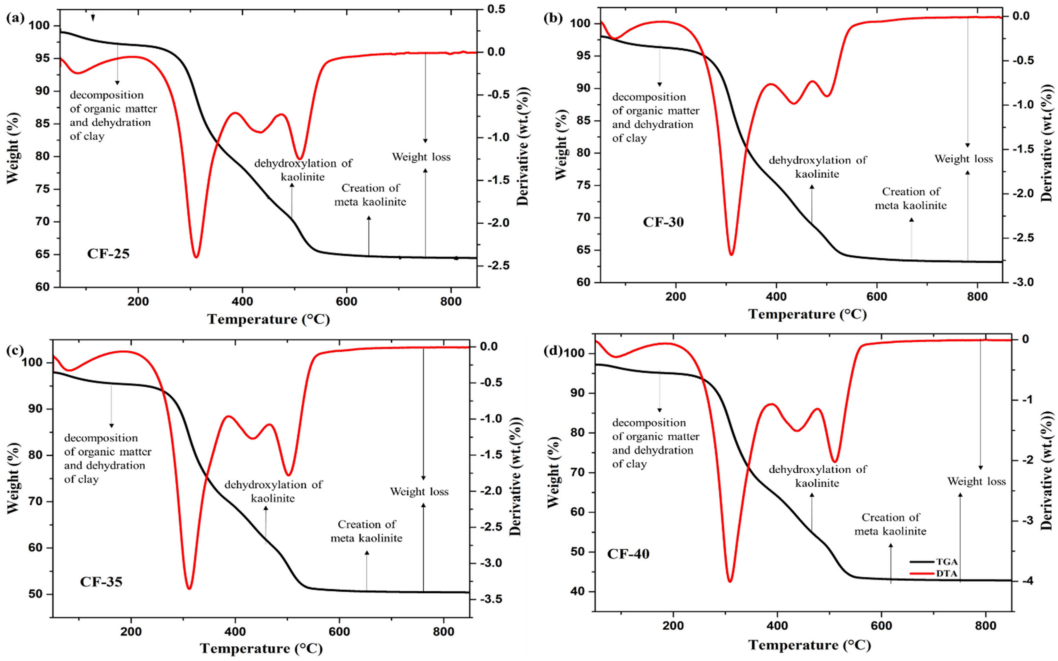

Figure 4. Thermal stability of (**a**) CF-25, (**b**) CF-30, (**c**) CF-35, and (**d**) CF-40.

3.1.6. Surface Charge of the Ceramic Filters

The CFs have large negative zeta potential values, indicating more stable colloids (Figure 5). Due to the isomorphic replacement of lower positive valence ions for the core Si and Al ions in the crystal lattice, kaolinite exhibits permanent negatively charged sites on the basal planes [33]. The ceramic matrix can be considered as a colloidal system whose stability is indicated by the magnitude of zeta potential. In addition, the electrophoretic mobility was negative, whereas conductivities were low (Table 2). The zeta potential has an influence on the fouling of CFs [34]. Negatively charged CFs have been reported to foul more when pollutants are positively charged and vice versa. Additionally, the sign on the zeta potential helps determine the reversibility of fouling [35]. Ionic interactions could be discounted as a potential MB and *o*-TB removal mechanism in this investigation, because ceramic filters had a negative surface charge which will facilitate the electrostatic attraction between the CF and the dyes [19].

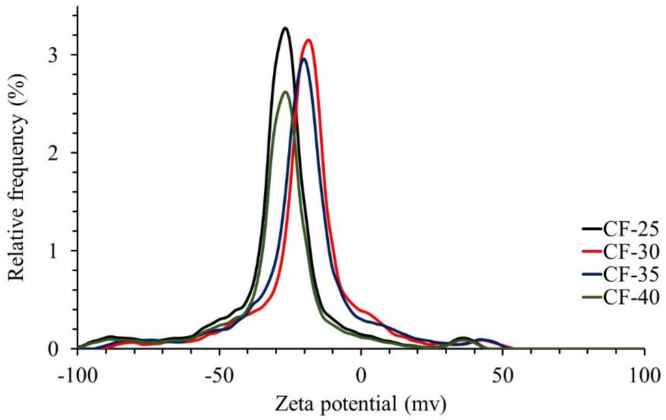

Figure 5. Zeta potential variation of ceramic filters.

Table 2. Zeta potential, electrophoretic mobility, and conductivity for CFs.

Ceramic Filter	Zeta Potential (mV)	Electrophoretic Mobility (μm·cm/V·s)	Conductivity (mS/cm)
CF-25	−26.8	−2.09	0.068
CF-30	−25.1	−1.95	0.072
CF-35	−27.8	−2.16	0.149
CF-40	−28.0	−2.28	0.180

3.1.7. Apparent Porosity, Water Adsorption, and Water Flow Rate of Ceramic Filters

The water adsorption for CF-25 and CF-30 was considerably lower than CF-35 and CF-40 (Table 3). This trend was anticipated, since CF-25 and CF-30 had lower content of coffee bean residues than CF-35 and CF-40, making them less porous. This is in line with earlier studies that found that the apparent porosity and water absorption increased as the amount of biomass material in the clay matrix increased [36]. Consequently, CF-40 had a higher water flow rate due to its higher porosity. The trend was consistent with earlier research showing that adding biomass or charcoal to CFs increases water flow rate [37]. A reduction in the content of coffee bean residues resulted in a reduction in water absorption (49.9%), apparent porosity (67.4%), and flow rate (10.4%). Increased apparent porosity and water absorption suggested increased permeability, both of which affected the water flow rates of the CFs [1]. Overall, the water flow rates monotonically declined with time in the CF.

Table 3. Water absorption, flow rate, and apparent porosity of ceramic filters.

Ceramic Filters	Water Absorption (%)	Flow Rate (L/h)	Apparent Porosity
CF-25	41.00 ± 0.82	1.28 ± 0.06	1.12 ± 0.03
CF-30	54.40 ± 1.02	1.50 ± 0.08	1.24 ± 0.08
CF-35	62.70 ± 1.92	2.20 ± 0.08	1.13 ± 0.02
CF-40	81.80 ± 1.99	3.93 ± 0.12	1.25 ± 0.02

3.2. Evaluation of Ceramic Filters in Removing Azo Dyes and Pathogens

3.2.1. Dye Removal Efficiency of the Ceramic Filters

The efficiency of CFs for MB removal was evaluated by passing contaminated water through the filters at atmospheric pressure under gravity, and the residual dye was monitored using UV-vis spectrophotometer. The maximum absorption peak around 662 nm, which corresponds to its hetero-polyaromatic linkage, is a characteristic peak of MB. As the filtration time increased, the absorption peak decreased, indicating progressive MB removal (Figure S1a–d). A notable blue shift was observed in the MB dye from 662 nm to 528 nm, which can be attributed to the dye being transformed to Azure B intermediates compounds [38]. Similarly, in the case of *o*-TB, the concentration of the dye reduced

over time (Figure S1e–h). While CF-25 completely reduced the dye concentration after 20 min (Figure S2e), CF-30 permeate was collected for 10 min (Figure S1f), CF-35 after 8 min (Figure S1g), and CF-40 after 120 s (Figure S1h). The spectra for *o*-TB exhibited a blue shift in wavelength from 635 nm to 522 nm, likely due to the dye being converted to diethylamine intermediates [39]. Both MB and *o*-TB absorption maxima decreased with time, indicating the progressive removal of the dyes. Despite the possible conversion of the azo dyes into intermediates, the removal efficiency increased with time.

CF-25 removed 59.21% of MB and *o*-TB by 92.72% (Figure S2a), while CF-30 (Figure S2b) effectively reduced MB by 42.99% and *o*-TB by 92.21%. Furthermore, CF-35 removed 59.74% of MB and *o*-TB by 85.85% (Figure S2c), while CF-40 effectively reduced MB by 43.84% and *o*-TB by 79.95% (Figure S2d). The overall removal of MB was in the range of 42.99–59.74%, while *o*-TB was in the range of 79.95–92.71% (Figure 6). CF-40 has a lower removal efficiency than CF-25, which can be attributed to the higher flow rate of CF-40. In addition to size exclusion, ionic interactions could be a possible removal mechanism for the organic dyes, because the ceramic filters' zeta potential of had a negative surface charge [40]. Overall, the modified ceramic filters demonstrated the capacity to reduce the concentration of MB and *o*-TB from the contaminated water.

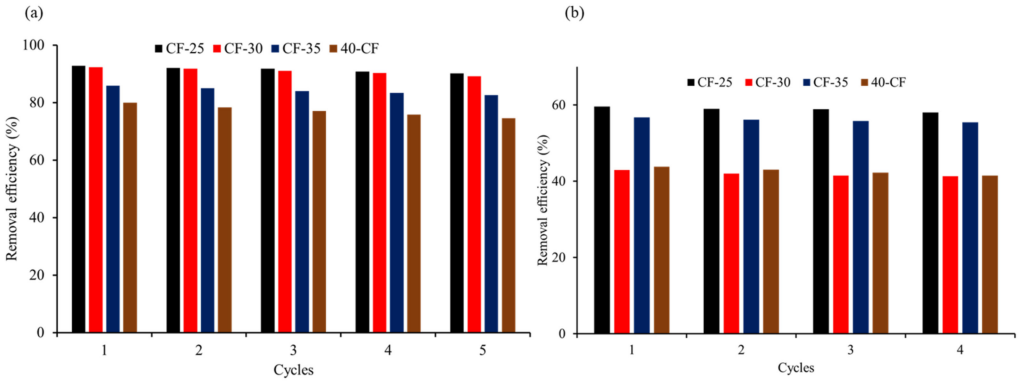

Figure 6. Recyclability of ceramic filters for (**a**) *o*-TB and (**b**) MB.

3.2.2. Recyclability of Ceramic Filters

The CFs retained about 88% of their removal capacity after four and five cycles for MB (Figure 6a) and *o*-TB (Figure 6b), respectively, indicating the CFs have high stability. The small decrease after each filtration cycle could be due to fouling, which clogged the pores, thereby reducing the porosity.

3.2.3. Removal of Pathogens

The antimicrobial activity of the ceramic filters against *S. aureus* and *S. typhi* was assessed by comparing the antimicrobial load in the feed and permeate. The initial concentration of *S. aureus* and *S. typhi* in the spiked feedwater was too numerous to count, which was evident from the highly dense colonies, even at 10^{-2} dilution (Figure 7). Filters CF-25 and CF-30 had the highest removal efficiency (100%) for the initial spiked feed water, while CF-35 had removal efficiency of 58% and 46% for *S. aureus* and *S. typhi*, respectively. Further 10^{-2} dilution increased the removal efficiency to 98% and 93%, respectively, after filtration. Filter CF-40 had a lower removal efficiency of 45% and 33% for *S. aureus* and *S. typhi*, respectively, and on further 10^{-2} dilution, the efficiency increased to 93% and 84%, respectively. A previous study reported the incomplete removal of *S. aureus* using pristine ceramic filters [41]. Contrastingly, complete removal of *S. aureus* and *S. typhi* was mostly by ceramic filters modified with silver nanoparticles [41,42]. The results show that the removal efficiency of CFs for pathogen removal are dependent on the clay content. It appears CFs with lower coffee beans residues and lower porosity, i.e., CF-25 and CF-30, have a high removal efficiency, and conversely higher coffee bean waste content and high porosity filters (i.e., CF-35 and CF-40) have a low removal efficiency. High filter porosity

is accompanied by a high water flow rate, which passes most bacterial organisms [36]. Overall, CFs were effective in removing *S. aureus* and *S. typhi* from contaminated water. The ability of the CFs to remove *S. aureus* and *S. typhi* could be attributed to the presence of antibacterial materials such as TiO_2 and SiO_2 in clay [43].

While the CFs in this study performed less than CFs modified with Ag nanoparticles, especially for the removal of pathogens [19], they are comparable to CFs fabricated from clay, sawdust, and diatomite [1], as well as others described in previous studies. In particular, clay ceramic pellets were 7.29% more effective in removing MB than the present filter [44]. However, in removing azo dyes, the present filter performed better compared to a filter fabricated from modified acid-activated kaolinite and TiO_2 [45]. The 100% *E. coli* removal effectiveness was comparable to that reported for candle type-ceramic filters [46], ceramic filters modified with silver nanoparticles [19], and low-cost ceramic filters [45]. The distinctions between the present filters and those described in the literature may be due to differing filter fabrication and operation conditions, such as filtration time and batch versus column operations. Interestingly, CFs had an excellent pathogen removal capacity, which negates the need for further modification using antimicrobial agents such as Ag nanoparticles. Further, the reusability over at least four cycles is an attractive property which could prolong the life span of the filters beyond the standard 2–3 years [19]. This should reduce the overall cost of the filters, while avoiding the risk of leaching Ag into the treated water.

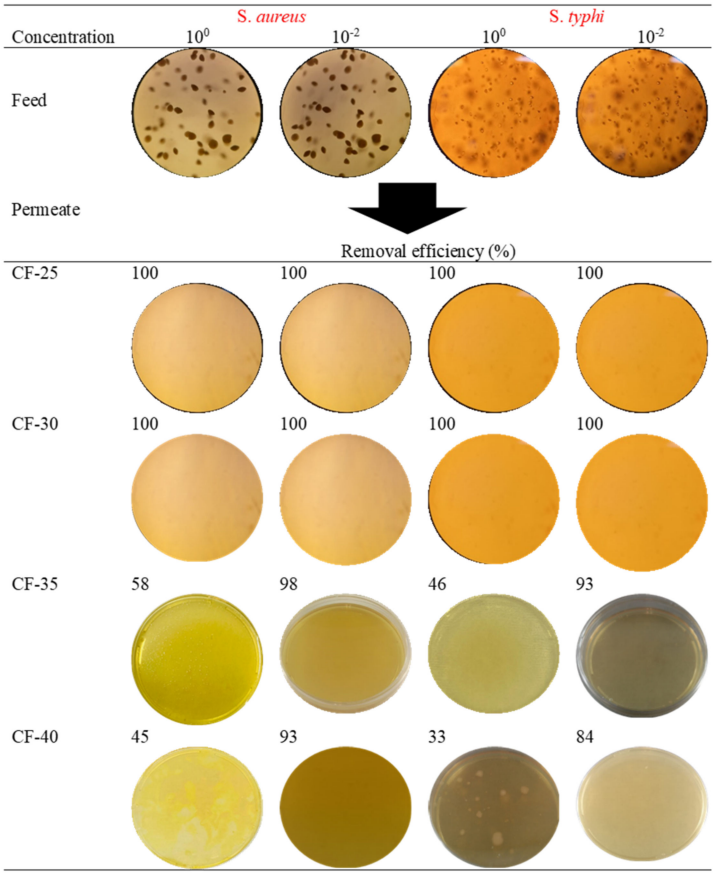

Figure 7. An illustration of *S. aureus* and *S. typhi* removal.

4. Conclusions

This study investigated the fabrication of low-cost pristine ceramic filters and evaluated them for the removal of methylene blue, *o*-toludine blue, *S. aureus*, and *S. typhi* from contaminated water. The fabrication involved use of locally available materials. The key findings were: (1) increased content of coffee bean residues increased the permeability of

the ceramic filters; (2) ceramic filters were effective and efficient in the removal of methylene blue (92.71%), *o*-toludine (59.74%), *S. aureus* (33–100%), and *S. typhi* (45–100%); (3) recyclability studies show the ceramic filters can be reused for at least four cycles without losing performance. These results show that ceramic filters can be used to replace expensive and complicated point-of-use water treatment techniques. In addition, there is expected to be a decrease in the overall cost of the filter, and there is no likelihood of Ag leaching into the permeate. Further studies should determine the chemical characteristics of the clay and filters using analytical techniques such as X-ray photoelectron spectroscopy and atomic force microscopy. The scaling up to pilot-scale, testing the acceptance of the devices by communities, and using environmentally relevant water samples, merit further research.

Supplementary Materials: The following supporting information can be downloaded at: https://www.mdpi.com/article/10.3390/ceramics6040131/s1. Figure S1: The removal efficiencies for MB and *o*-TB using ceramic filters. Figure S2: The removal efficiencies for MB and *o*-TB using ceramic filters.

Author Contributions: Conceptualization, N.C. and T.T.; methodology, N.C.; software, T.T.; validation, P.P.M., A.E.O.-S. and N.M.; formal analysis, M.O.; investigation, M.O. and A.E.O.-S.; resources, N.C. and N.M.; data curation, N.C.; writing—original draft preparation, M.O. and A.E.O.-S.; writing—review and editing, A.E.O.-S. and N.C.; visualization, N.C. and T.T.; supervision, N.C. and T.T.; project administration, N.C.; funding acquisition, N.C. and N.M. All authors have read and agreed to the published version of the manuscript.

Funding: This research was funded by NRF through the AJCORE grant (Grant No: 149019), and the APC was funded by Sol Plaatje University.

Data Availability Statement: The data presented in this study are available on request from the corresponding author.

Acknowledgments: The authors would like to acknowledge the support from the Risk and Vulnerability Research Centre, Sol Plaatje University.

Conflicts of Interest: The authors declare no conflict of interest.

References

1. Ekpunobi, U.; Agbo, S.; Ajiwe, V. Evaluation of the mixtures of clay, diatomite, and sawdust for production of ceramic pot filters for water treatment interventions using locally sourced materials. *J. Environ. Chem. Eng.* **2019**, *7*, 102791. [CrossRef]
2. Li, X.; Huang, G.; Li, Y.; Chen, X.; Yao, Y.; Liang, Y.; Huang, J.; Zhao, K.; Yin, J. Low-Cost ceramic disk filters coated with Graphitic carbon nitride (g-C3N4) for drinking water disinfection and purification. *Sep. Purif. Technol.* **2022**, *292*, 120999. [CrossRef]
3. WHO. 2017. Available online: https://www.who.int/news-room/fact-sheets/detail/diarrhoeal-disease (accessed on 2 August 2023).
4. WHO (World Health Organization). *Preventing Diarrhoea through Better Water, Sanitation and Hygiene: Exposures and Impacts in Low- and Middle-Income Countries*; World Health Organization: Geneva, Switzerland, 2014.
5. Muduli, M.; Choudhary, M.; Haldar, S.; Ray, S. Monitoring and assessment of Dracaena-based constructed vertical flow wetlands treating textile dye wastewater. *Environ. Monit. Assess.* **2022**, *194*, 727. [CrossRef]
6. López, A.; Rodríguez-Chueca, J.; Mosteo, R.; Gómez, J.; Rubio, E.; Goñi, P.; Ormad, M.P. How does urban wastewater treatment affect the microbial quality of treated wastewater? *Process Saf. Environ. Prot.* **2019**, *130*, 22–30. [CrossRef]
7. Maurya, A.; Singh, M.K.; Kumar, S. Biofiltration technique for removal of waterborne pathogens. In *Waterborne Pathogens*; Elsevier: Amsterdam, The Netherlands, 2020; pp. 123–141.
8. Ajala, O.; Tijani, J.; Salau, R.; Abdulkareem, A.; Aremu, O. A review of emerging micro-pollutants in hospital wastewater: Environmental fate and remediation options. *Results Eng.* **2022**, *16*, 100671. [CrossRef]
9. Solayman, H.; Hossen, M.A.; Abd Aziz, A.; Yahya, N.Y.; Hon, L.K.; Ching, S.L.; Monir, M.U.; Zoh, K.-D. Performance Evaluation Of Dye Wastewater Treatment Technologies: A Review. *J. Environ. Chem. Eng.* **2023**, *11*, 109610. [CrossRef]
10. Kali, A.; Amar, A.; Loulidi, I.; Hadey, C.; Jabri, M.; Alrashdi, A.A.; Lgaz, H.; Sadoq, M.; El-kordy, A.; Boukhlifi, F. Efficient adsorption removal of an anionic azo dye by lignocellulosic waste material and sludge recycling into combustible briquettes. *Colloids Interfaces* **2022**, *6*, 22. [CrossRef]
11. Zahid, M.; Ahmad, H.; Drioli, E.; Rehan, Z.A.; Rashid, A.; Akram, S.; Khalid, T. Role of polymeric nanocomposite membranes for the removal of textile dyes from wastewater. In *Aquananotechnology*; Elsevier: Amsterdam, The Netherlands, 2021; pp. 91–103.
12. Venugopal, V.; Sasidharan, A. Seafood industry effluents: Environmental hazards, treatment and resource recovery. *J. Environ. Chem. Eng.* **2021**, *9*, 104758. [CrossRef]

13. Jaber, L.; Elgamouz, A.; Kawde, A.N. An insight to the filtration mechanism of Pb (II) at the surface of a clay ceramic membrane through its preconcentration at the surface of a graphite/clay composite working electrode. *Arab. J. Chem.* **2022**, *15*, 104303. [CrossRef]
14. Hube, S.; Eskafi, M.; Hrafnkelsdóttir, K.F.; Bjarnadóttir, B.; Bjarnadóttir M, Á.; Axelsdóttir, S.; Wu, B. Direct membrane filtration for wastewater treatment and resource recovery: A review. *Sci. Total Environ.* **2020**, *710*, 136375. [CrossRef] [PubMed]
15. Farrow, C.; McBean, E.; Huang, G.; Yang, A.; Wu, Y.; Liu, Z.; Dai, Z.; Fu, H.; Cawte, T.; Li, Y. Ceramic water filters: A point-of-use water treatment technology to remove bacteria from drinking water in Longhai City, Fujian Province, China. *J. Environ. Inform.* **2018**, *32*, 63–68. [CrossRef]
16. Pérez-Vidal, A.; Rivera-Sanchez, S.P.; Florez-Elvira, L.J.; Silva-Leal, J.A.; Diaz-Gomez, J.; Herrera-Cuero, L.F.; Botero, L.P.L. Removal of *E. coli* and *Salmonella* in pot ceramic filters operating at different filtration rates. *Water Res.* **2019**, *159*, 358–364. [CrossRef]
17. Emenike, C.; Tenebe, I.; Omole, D.; Ngene, B.U.; Oniemayin, B.I.; Maxwell, O.; Onoka, B. Accessing safe drinking water in sub-Saharan Africa: Issues and challenges in South–West Nigeria. *Sustain. Cities Soc.* **2017**, *30*, 263–272. [CrossRef]
18. Chavoshani, A.; Hashemi, M.; Amin, M.M.; Ameta, S.C. *Micropollutants and Challenges: Emerging in the Aquatic Environments and Treatment Processes*; Elsevier: Amsterdam, The Netherlands, 2020.
19. Chaukura, N.; Katengeza, G.; Gwenzi, W.; Mbiriri, C.I.; Nkambule, T.T.; Moyo, M.; Kuvarega, A.T. Development and evaluation of a low-cost ceramic filter for the removal of methyl orange, hexavalent chromium, and *Escherichia coli* from water. *Mater. Chem. Phys.* **2020**, *249*, 122965. [CrossRef]
20. Rashad, D.; Amin, S.K.; Mansour, M.; Abdallah, H. Fabrication of low-cost antibacterial microfiltration tubular ceramic membranes. *Ceram. Int.* **2022**, *48*, 11489–11501. [CrossRef]
21. He, Y.; Huang, G.; An, C.; Huang, J.; Zhang, P.; Chen, X.; Xin, X. Reduction of *Escherichia coli* using ceramic disk filter decorated by nano-TiO_2: A low-cost solution for household water purification. *Sci. Total Environ.* **2018**, *616*, 1628–1637. [CrossRef]
22. Kassa, B.A.; Desta, A.F.; Assefa, F. Evaluating the efficacy of household filters used for the removal of bacterial contaminants from drinking water. *Afr. J. Microbiol. Res.* **2020**, *14*, 273–279.
23. Yang, H.; Min, X.; Xu, S.; Bender, J.; Wang, Y. Development of effective and fast-flow ceramic porous media for point-of-use water treatment: Effect of pore size distribution. *ACS Sustain. Chem. Eng.* **2020**, *8*, 2531–2539. [CrossRef]
24. Jagdale, P.; Ziegler, D.; Rovere, M.; Tulliani, J.M.; Tagliaferro, A. Waste coffee ground biochar: A material for humidity sensors. *Sensors* **2019**, *19*, 801. [CrossRef]
25. Song, P.N.; Mahy, J.G.; Calberg, C.; Farcy, A.; Caucheteux, J.; Fagel, N.; Lambert, S.D. Influence of thermal and acidic treatments on the morphology of a natural kaolinitic clay mineral. *Results Surf. Interfaces* **2023**, *12*, 100131. [CrossRef]
26. Zhang, B.; Huang, D.; Li, L.; Lin, M.; Liu, Y.; Fang, W.; Lu, J.; Liu, F.; Li, Y.; Liu, Y.; et al. Effect of magnesium salt contamination on the microstructures and properties of metakaolinitebased geopolymer: The role of $MgCl_2$ and $MgSO_4$. *J. Mater. Res. Technol.* **2022**, *20*, 4500–4514. [CrossRef]
27. Otieno, S.O.; Kengara, F.O.; Kemmegne-Mbouguen, J.C.; Langmi, H.W.; Kowenje, C.B.O.; Mokaya, R. The effects of metakaolinization and fused-metakaolinization on zeolites synthesized from quartz rich natural clays. *Microporous Mesoporous Mater.* **2019**, *290*, 109668. [CrossRef]
28. Kohout, J.; Koutnik, P.; Bezucha, P.; Kwocznski, Z. Leachability of the metakaolinite-rich materials in different alkaline solutions. *Mater. Today Commun.* **2019**, *21*, 10069. [CrossRef]
29. Dung TT, N.; Nam, V.N.; Nhan, T.T.; Hoang, B.N.; Hung DL, T.; Quang, D.V. Utilization of Rice Husk, an Abundant and Inexpensive Biomass in Porous Ceramic Membrane Preparation: A Crucial Role of Firing Temperature. *J. Nanomater.* **2021**, *2021*, 8688238. [CrossRef]
30. Wang, Z.; Peng, S.; Zhu, C.; Wang, B.; Du, B.; Cheng, T.; Jiang, Z.; Sun, L. Study of the denitration performance of a ceramic filter using a manganese-based catalyst. *RSC Adv.* **2023**, *13*, 344–354. [CrossRef] [PubMed]
31. Saja, S.; Bouazizi, A.; Achiou, B.; Ouaddari, H.; Karim, A.; Ouammou, M.; Aaddane, A.; Bennazha, J.; Younssi, S.A. Fabrication of low-cost ceramic ultrafiltration membrane made from bentonite clay and its application for soluble dyes removal. *J. Eur. Ceram. Soc.* **2020**, *40*, 2453–2462. [CrossRef]
32. Ahmad, R.; Aslam, M.; Park, E.; Chang, S.; Kwon, D.; Kim, J. Submerged low-cost pyrophyllite ceramic membrane filtration combined with GAC as fluidized particles for industrial wastewater treatment. *Chemosphere* **2018**, *206*, 784–792. [CrossRef]
33. Sangtam, A.R.; Saikia, P.; Goswamee, R.L.; Sinha, D.; Sinha, U.B. Green synthesis of mesoporous Ni-Co layered double hydroxide and its application for removal of 2, 4-dinitrophenol from water: A theoretical study complemented by the first principle density functional theory-Monte-Carlo approach. *J. Environ. Chem. Eng.* **2022**, *10*, 108378. [CrossRef]
34. Kassa, A.E.; Shibeshi, N.T.; Tizazu, B.Z. Kinetic analysis of dehydroxylation of Ethiopian kaolinite during calcination. *J. Therm. Anal. Calorim.* **2022**, *147*, 12837–12853. [CrossRef]
35. Manni, A.; El Haddar, A.; El Hassani, I.-E.E.A.; El Bouari, A.; Sadik, C. Valorization of coffee waste with Moroccan clay to produce a porous red ceramics (class BIII). *Boletín Soc. Española Cerámica Vidr.* **2019**, *58*, 211–220. [CrossRef]
36. Jiang, T.; Hirasaki, G.J.; Miller, C.A. Characterization of kaolinite ζ potential for interpretation of wettability alteration in diluted bitumen emulsion separation. *Energy Fuels* **2010**, *24*, 2350–2360. [CrossRef]
37. Howell, J.; Nyström, M. Fouling phenomena. In *Membranes in Bioprocessing: Theory and Applications*; Springer: Berlin/Heidelberg, Germany, 1993; pp. 203–241.

38. Huisman, I.H.; Trägårdh, G.; Trägårdh, C.; Pihlajamäki, A. Determining the zeta-potential of ceramic microfiltration membranes using the electroviscous effect. *J. Membr. Sci.* **1998**, *147*, 187–194. [CrossRef]
39. Bulta, A.L.; Micheal, G.A.W. Evaluation of the efficiency of ceramic filters for water treatment in Kambata Tabaro zone, southern Ethiopia. *Environ. Syst. Res.* **2019**, *8*, 1. [CrossRef]
40. Guleria, A.; Sharma, R.; Singh, A.; Upadhyay, N.K.; Shandilya, P. Direct dual-Z-scheme PANI/Ag_2O/Cu_2O heterojunction with broad absorption range for photocatalytic degradation of methylene blue. *J. Water Process Eng.* **2021**, *43*, 102305. [CrossRef]
41. Garrido, E.; Pla, L.; Lozano-Torres, B.; El Sayed, S.; Martínez-Máñez, R.; Sancenón, F. Chromogenic and fluorogenic probes for the detection of illicit drugs. *ChemistryOpen* **2018**, *7*, 401–428. [CrossRef] [PubMed]
42. Naeem, H.; Ajmal, M.; Qureshi, R.B.; Muntha, S.T.; Farooq, M.; Siddiq, M. Facile synthesis of graphene oxide–silver nanocomposite for decontamination of water from multiple pollutants by adsorption, catalysis and antibacterial activity. *J. Environ. Manag.* **2019**, *230*, 199–211. [CrossRef]
43. Bhan, C.; Golder, A.K. Utilizing Bioinspired AgNPs as an Antibacterial Agent to Enhance Ceramic Membrane Performance. *J. Environ. Chem. Eng.* **2023**, *11*, 110283. [CrossRef]
44. Luo, Y.; Liu, Z.; Wang, L.; Zhao, X.; Li, H.; Wu, M. High antibacterial and antioxidant cotton fabric based on AgNPs@ HTCS and hyaluronic acid via lay by lay self-assembly. *J. Ind. Text.* **2022**, *52*, 15280837221140922. [CrossRef]
45. Mustapha, S.; Oladejo, T.J.; Muhammed, N.M.; Saka, A.A.; Oluwabunmi, A.A.; Abdulkabir, M.; Joel, O.O. Fabrication of porous ceramic pot filters for adsorptive removal of pollutants in tannery wastewater. *Sci. Afr.* **2021**, *11*, e00705. [CrossRef]
46. Sharma, P.; Olufemi, A.F.; Qanungo, K. Development of green geo-adsorbent pellets from low fire clay for possible use in methylene blue removal in aquaculture. *Mater. Today Proc.* **2022**, *49*, 1556–1565. [CrossRef]

Disclaimer/Publisher's Note: The statements, opinions and data contained in all publications are solely those of the individual author(s) and contributor(s) and not of MDPI and/or the editor(s). MDPI and/or the editor(s) disclaim responsibility for any injury to people or property resulting from any ideas, methods, instructions or products referred to in the content.